A Scalable Mobile Multi-node Channel Sounder

Stefan Zelenbaba, David Löschenbrand, Markus Hofer, Anja Dakić,
Benjamin Rainer, Gerhard Humer, Thomas Zemen

Center for Digital Safety & Security, *AIT Austrian Institute of Technology GmbH*, Vienna, Austria,
stefan.zelenbaba@ait.ac.at

***Abstract*—The advantages of measuring multiple wireless links simultaneously has been gaining attention due to the growing complexity of wireless communication systems. Analyzing vehicular communication systems presents a particular challenge due to their rapid time-varying nature. Therefore multi-node channel sounding is crucial for such endeavors. In this paper, we present the architecture and implementation of a scalable mobile multi-node channel sounder. We perform a measurement campaign with three moving nodes, which includes a line of sight (LoS) connection on two links and non LoS (NLoS) conditions on the third link. We present the results on the obtained channel delay and Doppler characteristics, followed by the assessment of the degree of correlation of the analyzed channels and time-variant channel rates, hence investigating the suitability of the channel's physical attributes for relaying. The results show low cross-correlation between the transfer functions of the direct and the relaying link, while a higher rate is calculated for the relaying link.**

***Index Terms*—multi-node, 5G, wireless, channel sounding, V2V**

I. Introduction

The upcoming standards of 5$^{\text{th}}$ generation wireless communication networks (5G) and beyond 5G envision reliable link deployment in challenging environments, including vehicular and industrial scenarios. The traditional empirical methods for channel analysis, such as channel sounding involve one link between two nodes. However, due to the foreseen densification of connected nodes and the design of ultra-reliable systems, it has become clear that measuring multiple links simultaneously can provide a significant advantage on understanding the composite channel and saving time and effort on node redeployment or measurement repetitions.

Having that in mind, the concept of multi-link propagation, in both channel sounding and channel modeling has been attracting attention recently. A good overview of sounding methods, measurement campaigns and existing models is given in [1], including the summary of statistical models for cooperative relay channels.

The authors of [2] emphasize the need for measuring multiple channels simultaneously in an industrial environment. For this purpose, they develop a distributed multi-node multiple-input multiple-output (MIMO) channel sounding system. The nodes are synchronized by a centralized server, thus imposing an inherent limitation on the sounder's mobility.

An early version of a dynamic multi-node MIMO channel sounder capable of measuring dynamic links (with mobile nodes) is presented in [3] and used to measure an indoor channel in [4]. The sounder uses a single transmitter (Tx) node and two receiver (Rx) nodes, therefore covering two of the three links in the system.

An analysis of the coherence time and cross-correlation of the large-scale fading process between multiple vehicles in a highway scenario, done by measuring the received signal strength (RSSI), is presented in [5]. The authors of [5] then go a step further in [6] and [7] to model the shadowing and large-scale fading cross-correlation process, emphasizing the superiority of geometry based models in such scenarios.

Contributions of the Paper:

- To the best of our knowledge, we present the architecture for a scalable mobile multi-node channel sounder for the first time. The AIT multi-node channel sounder is able to capture high-resolution channel impulse responses of more than two rapidly time-variant wireless channels simultaneously.
- We describe the practical implementation of the proposed architecture with three nodes, optimized for robust vehicular measurements.
- To validate the sounder's functionality we perform a test measurement and characterize the recorded wireless channels in terms of delay and Doppler distribution.
- We justify the use of our channel sounder for vehicular relaying scenarios by examining the degree of correlation between the measured channels in terms of cross-correlation coefficients and comparing the time-variant channel rates of the direct and the relaying link.

II. Wireless Channel Sounding Principle

The channel sounding is done periodically with interval T, where every node can act either as a Tx or an Rx during one interval. In a system consisting of L nodes, we define the duration $T_{\text{sys}} = (L-1)T$, needed to sound all channels between all nodes, as a snapshot. During one snapshot we record a total of $W = L(L-1)/2$ channel transfer functions $g_{t,r}[m,q,k]$ corresponding to channels (t,r), where $t \in \{1,...,L\}$ and $r \in \{1,...,L\}$ for $t \neq r$, are the transmitting and receiving node indexes, respectively. Channel reciprocity is assumed such that $g_{t,r}[m,q,k] = g^*_{r,t}[m,q,k]$. Discrete time and frequency (subcarrier) indexes within one stationarity region are denoted by $m \in \{0,...,M-1\}$ and $q \in \{0,...,N-1\}$ respectively, while k denotes the stationarity region index [8].

The diagram of a full multi-node snapshot for a system of L nodes is depicted in Fig. 1.

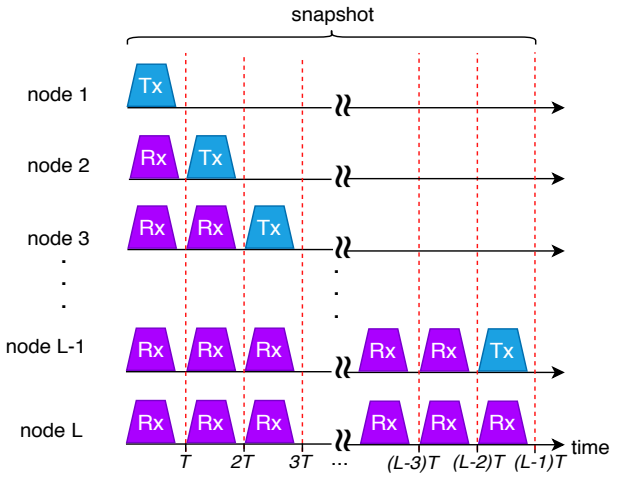

Fig. 1. Multi-node channel sounding diagram for a system of L nodes.

The total length T_{sys} increases with the number of nodes, which decreases the maximum resolvable Doppler shift. However, this concept allows a scalable and flexible implementation.

III. System Implementation

We use the National Instruments (NI) USRP software-defined radio (SDR) hardware as radio frequency (RF) frontend. LabView Communications software is used on the host PC of each node to control the triggering, sounding and data storage. A Rubidium oscillator clock is used to provide a 10 MHz frequency reference to the local oscillator, and a 1 pulse-per-second (1PPS) reference for snapshot synchronization. Each Rubidium oscillator includes a GPS receiver that feeds the polled GPS data to the host PC. To ensure synchronization on system level, all Rubidium clocks are synchronized to each other before the measurements. A real-time calculation of the channel transfer functions and channel impulse responses of all received channels allows for online evaluation.

Both available RF chains of the USRP are used to implement the Tx and Rx. We add a power amplifier (PA) on the Tx path and a bandpass filter on the Rx path, followed by a custom made AIT antenna switching unit. A block diagram depicting a single sounder node is shown in Fig. 2.

For a scenario with three nodes two Rx channels are measured within one snapshot. The different Rx channels have different gains, hence independent automatic gain control (AGC) settings are implemented for each Rx channel and updated using the field programmable gate array (FPGA) chip of the USRP.

In our implementation of the proposed mobile multi-node channel sounding concept, we use a system with $L = 3$ nodes and the sounding principle used in [9]. The orthogonal frequency division multiplex (OFDM) based sounding sequence

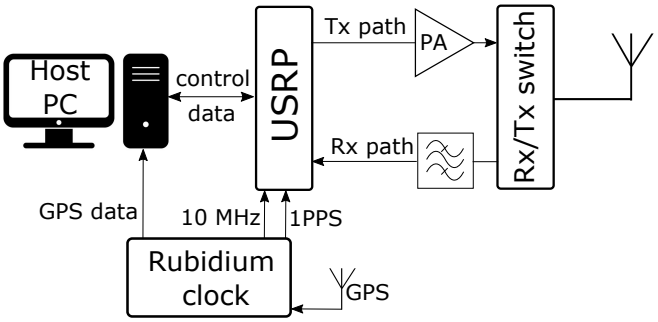

Fig. 2. A block diagram of one system node

consists of $N = 601$ subcarriers, spaced $\Delta f = 250\,\text{kHz}$ apart. The signal bandwidth is thus $B = 150\,\text{MHz}$, while the sampling rate of the Rx $f_{\text{s}} = 160\,\text{MHz}$. The sounding sequence has a duration of $12.8\,\mu\text{s}$, leaving the rest of the node snapshot duration to be used for switching, AGC setting, buffer clearing and data storage. The sounding interval is set to $T = 250\,\mu\text{s}$, making the snapshot rate $T_{\text{sys}} = 500\,\mu\text{s}$.

Before each measurement, a back-to-back (B2B) calibration is done using an attenuated direct cable connection, to determine and omit the impact of RF components from the measurements, as well as to ensure channel reciprocity.

IV. Channel Characterization

The Rx nodes record raw I and Q data to estimate the discrete channel transfer function $g_{t,r}[m, q, k]$. We calculate the local scattering function (LSF) [10] as a multi-taper estimate [11] of the scattering function, for each $M \times N$ sized stationarity region k. The LSF is obtained with the stationarity region length of $T_{\text{stat}} = 120\,\text{ms}$ in time and 150 MHz in frequency [8], through [12]

$$\hat{C}_{t,r}[k; n, p] = \frac{1}{IJ} \sum_{w=0}^{IJ-1} |\mathcal{H}_{t,r}^{(G_w)}[k; n, p]|^2 \,, \tag{1}$$

where $\mathcal{H}^{(G_w)}$ presents the windowed time-variant frequency response, defined as

$$\mathcal{H}_{t,r}^{(G_w)}[k; n, p] = \sum_{m'=M/2}^{M/2-1} \sum_{q'=-(N-1)/2}^{(N-1)/2} g_{t,r}[m' - m, q' - q, k] G_w[m', q', k] e^{-\text{j}2\pi(pm' - nq')} \,, \tag{2}$$

with $n \in \{0, ..., N-1\}$ and $p \in \{-M/2, ..., M/2-1\}$ being the delay and Doppler shift indexes, respectively. The window function $G_w[m', q', k] = u_i[m' + M/2]\tilde{u}_j[q' + N/2]$ uses band-limited discrete prolate spheroidal sequences (DPSS) [13] u_i, indexed with $i \in \{0, ..., I-1\}$, and u_j, indexed with $j \in \{0, ..., J-1\}$, while $w = iJ + j$.

We calculate the time-variant power delay profile (PDP) and Doppler spectral density (DSD) using the LSF as

$$\hat{P}_{\tau;\,t,r}[k; n] = \frac{1}{M} \sum_{p=-M/2}^{M/2-1} \hat{C}_{t,r}[k; n, p] \,, \tag{3}$$

and

$$\hat{P}_{\nu;\,t,r}[k;p] = \frac{1}{N}\sum_{n=0}^{N-1}\hat{C}_{t,r}[k;n,p]\,. \tag{4}$$

We use the PDP and DSD to observe the received power that arrives within each delay and Doppler bin, respectively, and get a better understanding of the impact of the environment on signal propagation.

Delay and Doppler dispersion of the channel can be described by the root mean square (RMS) delay spread and RMS Doppler spread, respectively. They are calculated as

$$\sigma_{\tau;\,t,r}[k] = \sqrt{\frac{\sum_{n=0}^{N-1}(n\tau_\mathrm{s})^2\hat{P}_{\tau;\,t,r}[k;n]}{\alpha_{t,r}[k]} - \bar{\tau}_{t,r}[k]^2}\,, \tag{5}$$

where $\tau_\mathrm{s} = 1/B = 6.67\,\mathrm{ns}$ is the delay bin width while

$$\bar{\tau}_{t,r}[k] = \frac{\sum_{n=0}^{N-1}(n\tau_\mathrm{s})\hat{P}_{\tau;\,t,r}[k;n]}{\alpha_{t,r}[k]}\,, \text{and} \tag{6}$$

$$\alpha_{t,r}[k] = \sum_{n=0}^{N-1}\hat{P}_{\tau;\,t,r}[k;n] = \sum_{p=-M/2}^{M/2-1}\hat{P}_{\nu;\,t,r}[k;p]\,, \tag{7}$$

are the mean delay and the channel gain, respectively. The RMS Doppler spread is calculated as

$$\sigma_{\nu;\,t,r}[k] = \sqrt{\frac{\sum_{p=-M/2}^{M/2-1}(p\nu_\mathrm{s})^2\hat{P}_{\nu;\,t,r}[k;p]}{\alpha_{t,r}[k]} - \bar{\nu}_{t,r}[k]^2}\,, \tag{8}$$

where $\nu_\mathrm{s} = 1/T_\mathrm{stat} = 8.33\,\mathrm{Hz}$ is the minimal resolvable Doppler shift, and

$$\bar{\nu}_{t,r}[k] = \frac{\sum_{p=-M/2}^{M/2-1}(p\nu_\mathrm{s})\hat{P}_{\nu;\,t,r}[k;p]}{\alpha_{t,r}[k]}\,, \tag{9}$$

the mean Doppler shift.

We use the power threshold criterion [14] in the calculations, such that any spurious noise components 5 dB above the noise floor, and weak multi-path components (MPCs) 40 dB below the peak value, are omitted from the calculations.

To investigate the degree of correlation between the measured channels, we obtain the time-variant cross-correlation coefficients between channels (t,r) and (t',r') as

$$\rho_{t,r;\,t',r'}[k] = \frac{1}{N}\sum_{q=0}^{N-1}\frac{C_{t,r;\,t',r'}[q,k]}{\sigma_{t,r}[q,k]\sigma_{t',r'}[q,k]}\,, \tag{10}$$

where

$$C_{t,r;\,t',r'}[q,k] = \frac{1}{M}\sum_{m=0}^{M-1}(g_{t,r}[m,q,k]-\mu_{t,r}[q,k]) \\ (g_{t',r'}[m,q,k]-\mu_{t',r'}[q,k])^*\,, \tag{11}$$

is the covariance between channels (t,r) and (t',r'). The sample variance and sample mean of channel (t,r) are calculated as

$$\sigma^2_{t,r}[q,k] = \frac{1}{M}\sum_{m=0}^{M-1}|g_{t,r}[m,q,k]-\mu_{t,r}[m,q]|^2\,, \text{and} \tag{12}$$

$$\mu_{t,r}[q,k] = \frac{1}{M}\sum_{m=0}^{M-1}g_{t,r}[m,q,k]\,, \tag{13}$$

respectively.

V. Measurement Setup

To validate the sounder operation and justify it's use for the relaying use case, we perform a single-input single-output (SISO) measurement with changing LoS and NLoS conditions, which can be easily translated to vehicular or industrial scenarios.

The test scenario is depicted in Fig. 3. Node 1 is kept static on one side of the building while nodes 2 and 3 are placed behind the corner, having NLoS conditions with node 1. Nodes 2 and 3 are mounted on hand-pushed trolleys and moving behind each other, maintaining a distance of $d \approx 5\,\mathrm{m}$. As node 3 goes around the corner first to establish a LoS connection with node 1, node 2 remains shadowed by the building while at the same time maintaining a strong LoS with node 3. During this period, NLoS conditions exist on one link, while the other two links have LoS conditions.

The carrier frequency of 5.9 GHz is used due to it's planned use in vehicular applications. Each node uses an omnidirectional dipole antenna with 4 dBi gain. A summary of the measurement parameters is given in Table I.

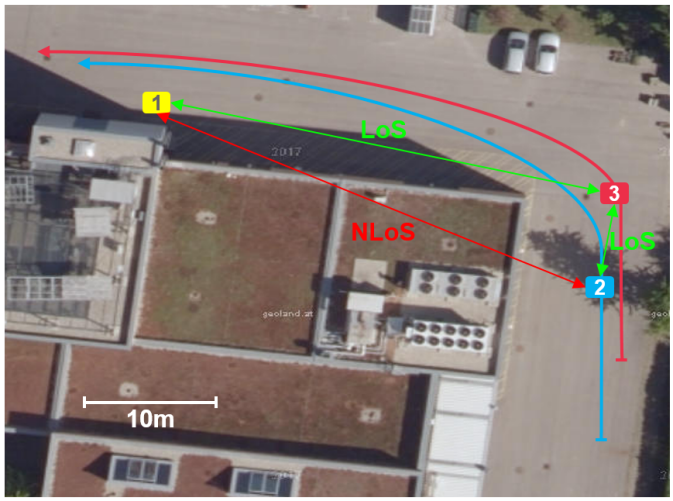

Fig. 3. Test scenario diagram with node trajectories (map source: geoland.at)

VI. Results

A comparison of the obtained PDPs is shown in Fig. 4. Link $(2,3)$ maintains a high signal to noise ratio (SNR), while link $(1,3)$ shows an emerging LoS component starting from $t_1 \approx 7.2\,\mathrm{s}$ and link $(1,2)$ remains in poor channel conditions

TABLE I
CHANNEL SOUNDING PARAMETERS

Parameter	Value
Configuration	SISO
Carrier frequency	5.9 GHz
Measurement Bandwidth	150 MHz
Node Snapshot Interval	250 μs
System Snapshot Interval	500 μs

due to the obstruction of the building until $t_2 \approx 15.6\,\mathrm{s}$. This is also in line with the gathered GPS data. The additional paths seen in the PDPs come from static scatterers such as parked cars. The comparison of the obtained DSDs is shown in Fig. 5. The specular components reach $\approx 33\,\mathrm{Hz}$ Doppler shifts corresponding to the velocity of $\approx 1.68\,\mathrm{m/s}$.

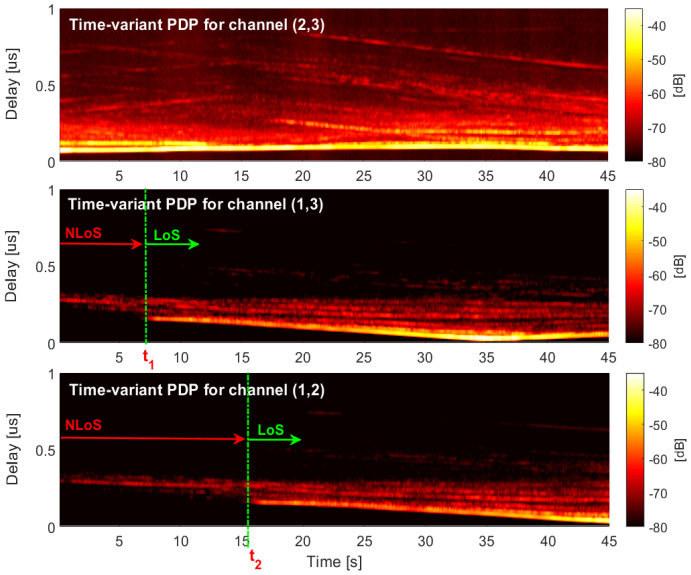

Fig. 4. PDP comparison of channels $(2,3)$, $(1,3)$ and $(1,2)$

Due to the low speed of the nodes, neither of the links show high RMS Doppler spreads, while RMS delay spreads get more stable as the LoS conditions improve for each link.

The channel gains (7) depicted in Fig. 7 show that during the time period $\Delta t = t_2 - t_1$ link $(1,3)$ is more than $10\,\mathrm{dB}$ stronger than link $(1,2)$ due to the presence of LoS conditions between nodes 1 and 3. Therefore node 3 can be potentially used as a relay node between 1 and 2, in order to convey safety critical information. In that case, channels $(1,3)$ and $(2,3)$ would act as parts of the relay link, and channel $(1,2)$ as a direct link.

Fig. 7 also shows the obtained cross-correlation coefficients (10) between the relay links and the direct link. Before time instant t_1, there is some cross-correlation between channels $(1,3)$ and $(1,2)$ since they are both in NLoS from node 1. The compared links then exhibit very low cross-correlation coefficient values during Δt, which is expected due to different propagation conditions. After time t_2, all three channels have LoS conditions, and as the distance between nodes decreases, the cross-correlation coefficients grow.

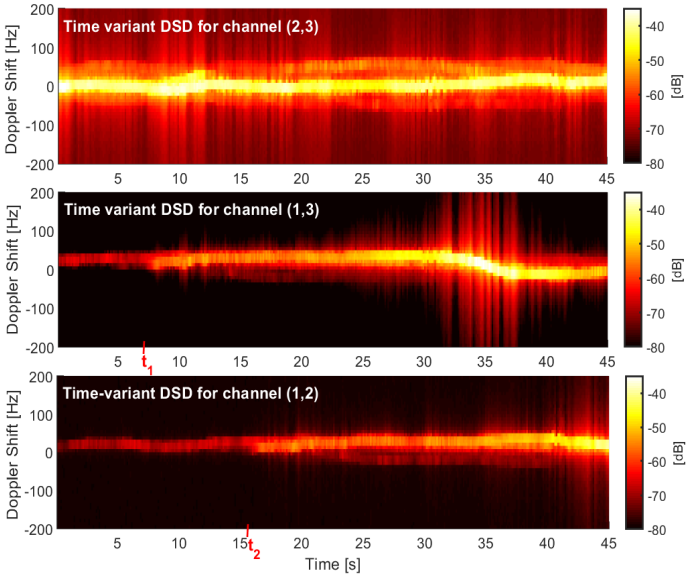

Fig. 5. DSD comparison of channels $(2,3)$, $(1,3)$ and $(1,2)$

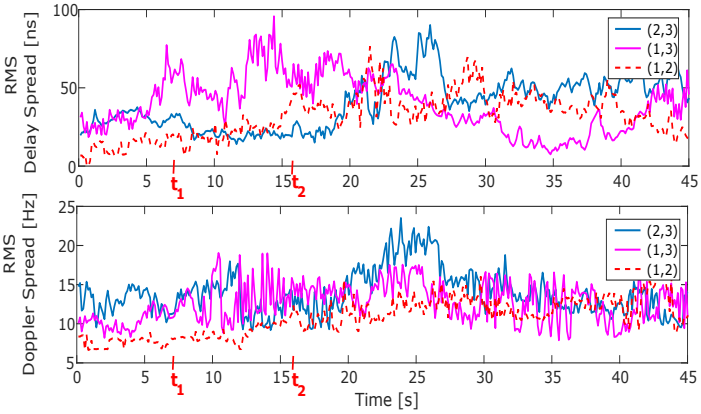

Fig. 6. RMS delay and Doppler spread of all three links over time

To illustrate the benefit of using node 3 as a relay instead of node 1 transmitting directly to node 2, we compare the time-variant channel rates of the direct link and the relay link.

Since the sounding of different channels is done independently, we assume a simple half-duplex multi-hop decode-and-forward relaying scheme. Therefore, to calculate the time-variant channel rate of link (t,r) for each stationarity region, we use [15]

$$R_{t,r}[k] = \frac{1}{2MN} \sum_{q=0}^{N-1} \sum_{m=0}^{M-1} \log_2\left(1 + \frac{|g_{t,r}[m,q,k]|}{\gamma}\right). \quad (14)$$

Since the variation in SNR is contained within the channel transfer functions, for the purpose of this comparison we use a fixed channel gain normalization factor γ, corresponding to $-60\,\mathrm{dB}$.

The time-variant rate of the multi-hop relay channel is then obtained as

$$R_{\mathrm{relay}}[k] = \min\left\{R_{1,3}[k], R_{2,3}[k]\right\}. \quad (15)$$

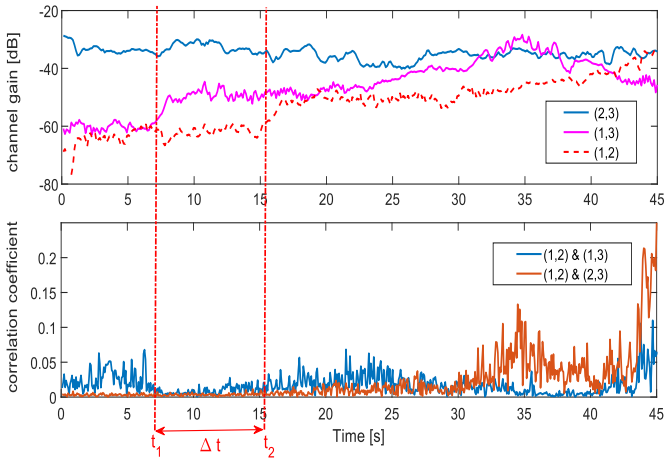

Fig. 7. Channel gains and cross-correlation coefficients between the direct and the relay channels

The calculated rates are directly connected to the SNR of the channels, with the lower SNR of the relay links being the bottleneck. Fig. 8 shows the calculated comparison of the time-variant channel rates of the direct and the relay link. The relay link (2,3,1) performs better shortly after t_1 as node 3 obtains a LoS link with node 1. As node 2 emerges to obtain LoS with node 1 at time t_2, the direct link rate gains on the relay link rate, but then again keeps at a lower rate as node 2 goes again behind and is shadowed by node 3. As they both pass node 1, node 3 is shadowed by node 2 and R_{relay} drops below $R_{1,2}$.

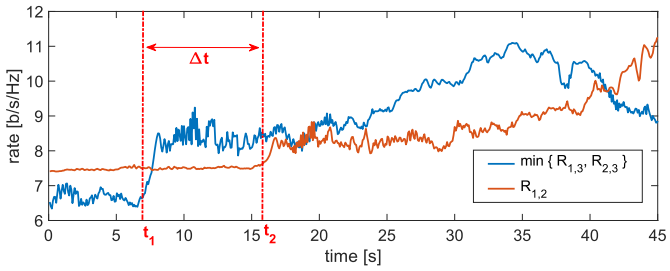

Fig. 8. Comparison of the time-variant channel rates for the direct link (1,2) and the relay link (2,3,1).

VII. Conclusions

In this paper we present a scalable mobile multi-node channel sounder architecture, able to measure links between more than two nodes at high temporal snapshot rates. We describe the hardware implementation of the proposed architecture and provide first field measurement data with three nodes, thus demonstrating the envisioned relaying use case for vehicular communications in intelligent transportation systems. A stochastic characterization of the channel by means of PDP, DSD, RMS delay and Doppler spread from the measurement data is obtained. The collected data is suitable to derive and parametrize a geometry-based stochastic channel model for a system consisting of more than two nodes. We also investigate the degree of correlation between the direct and the relaying channels by means of calculating the cross-correlation coefficients, and afterwards compare the links in terms of achieved channel rates. By validating the proposed multi-node sounding concept, we justify future vehicular measurements for realistic use cases, as they can provide a thorough insight in the complex propagation conditions of such systems. The presented system can be further expanded to support MIMO operation with N_{T} transmit and N_{R} receive antennas, by sounding the channels of individual antenna pairs according to the switched array principle. The implementation of novel antenna switching approaches in channel sounding, such as the one used in [16] can be investigated in more detail in order to increase the maximum resolvable Doppler shifts for vehicular scenarios.

Acknowledgements

The measurement campaign described in the paper was done as a part of project SCOTT (www.scott-project.eu) that has received funding from the Electronic Component Systems for European Leadership (ECSEL) Joint Undertaking under grant agreement No 737422. This joint undertaking receives support from the European Unions Horizon 2020 research and innovation programme, and Austria, Spain, Finland, Ireland, Sweden, Germany, Poland, Portugal, Netherlands, Belgium, Norway.

References

[1] C. Oestges, "Multi-link propagation modeling for beyond next generation wireless," in *2011 Loughborough Antennas Propagation Conference (LAPC), 2011 Loughborough, UK*, Nov 2011, pp. 1–8.

[2] D. A. Wassie, I. Rodriguez, G. Berardinelli, F. M. L. Tavares, T. B. Sørensen, T. L. Hansen, and P. Mogensen, "An agile multi-node multi-antenna wireless channel sounding system," *IEEE Access*, vol. 7, pp. 17 503–17 516, 2019.

[3] P. Almers, K. Haneda, J. Koivunen, V.-M. Kolmonen, A. Molisch, A. Richter, J. Salmi, F. Tufvesson, and P. Vainikainen, "A dynamic multi-link MIMO measurement system for 5.3 GHz," *in Proc. 29th URSI General Assembly, Chicago, USA, Aug. 2008.*, 01 2008.

[4] J. Koivunen, P. Almers, V. . Kolmonen, J. Salmi, A. Richter, F. Tufvesson, P. Suvikunnas, A. F. Molisch, and P. Vainikainen, "Dynamic multi-link indoor MIMO measurements at 5.3 GHz," in *The Second European Conference on Antennas and Propagation, EuCAP 2007*, Nov 2007, pp. 1–6.

[5] M. G. Nilsson, D. Vlastaras, T. Abbas, B. Bergqvist, and F. Tufvesson, "On multilink shadowing effects in measured V2V channels on highway," in *2015 9th European Conference on Antennas and Propagation (EuCAP)*, April 2015, pp. 1–5.

[6] M. G. Nilsson, C. Gustafson, T. Abbas, and F. Tufvesson, "A measurement-based multilink shadowing model for V2V network simulations of highway scenarios," *IEEE Transactions on Vehicular Technology*, vol. 66, no. 10, pp. 8632–8643, Oct 2017.

[7] C. A. T. T. F. Nilsson, M.G.; Gustafson, "A path loss and shadowing model for multilink vehicle-to-vehicle channels in urban intersections," *Sensors 18, 4433.*, 2018.

[8] L. Bernadó, T. Zemen, F. Tufvesson, A. F. Molisch, and C. F. Mecklenbräuker, "The (in-) validity of the WSSUS assumption in vehicular radio channels," in *2012 IEEE 23rd International Symposium on Personal, Indoor and Mobile Radio Communications - (PIMRC)*, Sep. 2012, pp. 1757–1762.

[9] S. Zelenbaba, L. W. Mayer, E. Mozo, F. Wirth, R. Hladik, A. Alonso, L. Bernad, M. Schiefer, and T. Zemen, "Characterization of time-variant wireless channels in railway communication scenarios," in *2019 IEEE 2nd 5G World Forum (5GWF) (WF-5G'19)*, Desdren, Germany, Sep. 2019.

[10] G. Matz, "On non-WSSUS wireless fading channels," *IEEE Transactions on Wireless Communications*, vol. 4, no. 5, pp. 2465–2478, Sep. 2005.

[11] D. J. Thomson, "Spectrum estimation and harmonic analysis," vol. 70, no. 9, pp. 1055 – 1096, September 1982.
[12] L. Bernadó, T. Zemen, F. Tufvesson, A. F. Molisch, and C. F. Mecklenbräuker, "Delay and Doppler spreads of nonstationary vehicular channels for safety-relevant scenarios," *IEEE Transactions on Vehicular Technology*, vol. 63, no. 1, pp. 82–93, Jan 2014.
[13] D. Slepian, "Prolate spheroidal wave functions, fourier analysis, and uncertainty — v: the discrete case," *The Bell System Technical Journal*, vol. 57, no. 5, p. Slepian78, May 1978.
[14] N. Czink, "The random-cluster model – a stochastic MIMO channel model for broadband wireless communication systemsof the 3rd generation and beyond," Ph.D. dissertation, TU Wien, Vienna, 2007.
[15] A. F. Molisch, *Wireless Communications*. John Wiley & Sons, 2010.
[16] R. Wang, O. Renaudin, C. U. Bas, S. Sangodoyin, and A. F. Molisch, "On channel sounding with switched arrays in fast time-varying channels," *IEEE Transactions on Wireless Communications*, vol. 18, no. 8, pp. 3843–3855, Aug 2019.